LA-UR- 98-2871

CONF-981138--

Comparison of a Diagnostic Wildfire Modeling System (HIGRAD/BEHAVE) With a Self-Determining Wildfire Modeling System (HIGRAD/FIRETEC)

By

Jon Reisner, Rodman Linn, and James Bossert

Los Alamos National Laboratory
Los Alamos, New Mexico 87544
email:reisner@lanl.gov

SUMMARY

In this paper details of our wildfire modeling system are illustrated. First our dynamical model, HIGRAD, capable of accurately resolving regions of strong gradients is described. Next, our two wildfire models FIRETEC and BEHAVE are introduced. Unlike the traditional point-functional approach used in our BEHAVE-like fire model, FIRETEC is a self-determining fire model. The benefits of the HIGRAD/FIRETEC approach with respect to HIGRAD/BEHAVE are shown in the results section of this paper. Two major conclusions are drawn in this section. The first conclusion is that the rate of spread of a fire to a first approximation is independent of the local wind velocity. The second conclusion is that HIGRAD/FIRETEC can be used to develop point-functions for use in HIGRAD/BEHAVE.

INTRODUCTION

The ability to accurately forecast the spread of a wildfire would significantly reduce human suffering and loss of life, the destruction of property, and expenditures for assessment and recovery. To help achieve this goal we have developed a model which accurately simulates the interactions between winds and the heat source associated with a wildfire. We have termed our new model HIGRAD or a HIgh resolution model for strong GRADient applications. HIGRAD employs sophisticated numerical techniques to prevent numerical oscillations from occurring in the vicinity of the fire. As well, HIGRAD uses a numerical technique which enables the compressible equation set to be solved to an accuracy of second-order, but using a time step which is not governed by the speed of sound.

HIGRAD has been previously linked to a BEHAVE-like fire model (Reisner et al. 1998; Andrews 1986; Andrews and Chase 1989). The fire model uses empirical functions (Rothermel 1972, 1991) to determine the rate of fire spread. By design the BEHAVE model is computationally efficient; however, whether a simple empirical model can accurately forecast fire spread is somewhat debatable. For example, the rates of spread

DISCLAIMER

DISCLAIMER

Portions of this document may be illegible in electronic image products. Images are produced from the best available original document.

that appear in BEHAVE were primarily developed by examining experimental fires in a wind tunnel. The fuel beds used in the wind tunnels and the upstream wind speeds (U<3 m s^{-1}) for which wind tunnel experiments remain valid are not typically what is present in a realistic wildfire (Catchpole et al. 1998). Another major difficulty in employing a BEHAVE-type fire model is determining where the upstream wind should be measured. Should the wind speed be taken far upstream of the fire or should the upstream wind speed represent some average wind velocity just upstream of the fire front? In our previous simulation of the tragic South Canyon fire near Glenwood Springs Colorado (Reisner et al. 1998; Rosenkrance et al. 1994) we have assumed the later.

The development of FIRETEC (Linn 1997; Linn and Harlow 1998), a self-determining fire model, was an important first step towards reducing the fire communities reliance on a point-functional model to describe a wildfire's movement. An immediate benefit of FIRETEC is that the fire spread is no longer a direct function of windspeed. Instead the fire spread rate is a function of variables such as the density of fuel, the density of oxygen, and the turbulence intensity. And, unlike the wind tunnel experiments, FIRETEC can be used for wind speeds > 3 m s^{-1}. In this paper we intend to demonstrate how FIRETEC can be used to improve our BEHAVE-like fire model. In the next three sections we will describe HIGRAD and the two fire modules. We will next present results from HIGRAD/FIRETEC and HIGRAD/BEHAVE. Finally, we present some concluding remarks and our future plans.

HIGRAD

HIGRAD solves the compressible form of the Navier-Stokes equations. The turbulence parameterization used in this version of HIGRAD are based upon Linn's (1997) multiscale turbulence approach. In this approach three different relevant size scales for the turbulence associated with the wildfire are parameterized. The largest of the relevant size scales, A scales, is the size of the largest fuel structures. The next largest scales are the B scales, which are associated with the distance between branches. C scales are the smallest and are associated with scales at the size of the small structures of the fuel, such as leaves or pine needles. The multiscale turbulence approach is active during either a HIGRAD/BEHAVE simulation or a HIGRAD/FIRETEC simulation. The flux-form representation of the Navier-Stokes equations can be expressed as follows:

$$\frac{\partial G u \rho}{\partial t} + \nabla \cdot (\mathbf{v} G \rho u) = G R_x \tag{1a}$$

$$\frac{\partial G v \rho}{\partial t} + \nabla \cdot (\mathbf{v} G \rho v) = G R_y \tag{1b}$$

$$\frac{\partial G w \rho}{\partial t} + \nabla \cdot (\mathbf{v} G \rho w) = G R_z \tag{1c}$$

$$\frac{\partial GI\rho}{\partial t} + \nabla \cdot (\mathbf{v}GI\rho) = GR_I \tag{1d}$$

$$\frac{\partial G\rho}{\partial t} + \nabla \cdot (\mathbf{v}G\rho) = R_\rho \tag{1e}$$

$$p = \rho R_d T \tag{1f}$$

where u, v, and w are the velocity components in the coordinate system $[x, y, z] = [x_c, y_c, z_c]$ with the subscript c referring to Cartesian coordinates, I is the internal energy of the gas, ρ is the density, $G = Det\{\ \partial \mathbf{x_c}/\partial \mathbf{x}\} = (Det\{\ G^{IJ}\}\ )^{-1/2}$ is the Jacobian of transformation with $G^{IJ} = \sum_{K=1}^{3} (\partial x^I/\partial x_c^K)(\partial x^J/\partial x_c^K)$. (1f) is an equation relating the total pressure, p, to variable ρ and the temperature of the gas. The temperature of the gas, T, is related to the internal energy by the following relationship,

$$I = C_v T \tag{1g}$$

. The constants, $C_v = 717$ J K^{-1} kg^{-1} and and $R_d = 287$ J K^{-1} kg^{-1}, in (1f) and (1g) are the specific heat of air at constant volume and the gas constant of dry air. The contravariant vertical component of the advective velocity vector $\mathbf{v} = u\hat{i} + v\hat{j} + \omega\hat{k}$ which appears as the result of employing a terrain-following coordinate system, $[x, y, andz] = [x_c, y_c, H(z_c - h)/(H - h)]$ with H being the model depth and $h = h(x_c, y_c)$ the model bottom, can be related to the cartesian velocity components by the following relationship, $\omega = G^{13}u + G^{23}v + G^{-1}w$.

The forces R_x, R_y, R_z, R_I, and R_ρ in (1) are expressed as follows:

$$\begin{aligned} R_x = &- \frac{\partial p'}{\partial x} - G^{13}\frac{\partial p'}{\partial z} + f\rho(v - v_e) - \hat{f}\rho(w - w_e) - \\ &\alpha_a\rho(u - u_e) - D\rho u - \frac{\partial R_{1j}}{\partial x_j} \end{aligned} \tag{2a}$$

$$R_y = -\frac{\partial p'}{\partial y} - G^{23}\frac{\partial p'}{\partial z} - f\rho(u - u_e) - \alpha_a\rho(v - v_e) - D\rho v - \frac{\partial R_{2j}}{\partial x_j} \tag{2b}$$

$$R_z = -G^{-1}\frac{\partial p'}{\partial z} - \rho' g + \hat{f}\rho(u - u_e) - \alpha_a\rho(w - w_e) - D\rho w - \frac{\partial R_{3j}}{\partial x_j} \tag{2c}$$

$$R_I = -\alpha_a(\theta - \theta_e) + \frac{\partial}{\partial x_i}\left[\sigma_{cij}\frac{\partial I}{\partial x_j}\right] + H \tag{2d}$$

$$R_\rho = -\alpha_a(\rho - \rho_e) \tag{2e}$$

where u_e, v_e, and w_e are the balanced environmental velocity components, $f = 2\Omega sin\varphi$ and $\hat{f} = 2\Omega cos\varphi$ are the z and y components of the Earth rotation vector at the latitude φ, g is the acceleration due to gravity, and $\rho' = \rho - \rho_e$ is the density perturbation with

$\rho_e = \rho_e(z_c)$ the environmental density, H is the heat source (described in the next two sections) associated with the wildfire, and the damping forcings appearing in (2) being used to simulate wave-absorbing regions and/or nudging (Davies 1983). In (2a)-(2c) $p' = p - p_e$ is the pressure perturbation with the environmental pressure, p_e, being calculated using (1f).

The terms $\frac{\partial R_{ij}}{\partial x_j}$ appearing in (2a)-(2c) are associated with the divergence of the total Reynolds stresses of all turbulence scales $R_{ij} = R_{ij_A} + R_{ij_B} + R_{ij_C}$. R_{ij_A} is calculated from the following expression

$$R_{ij_A} = -\rho v_t \left(\frac{\partial u_i}{\partial x_j} + \frac{\partial u_j}{\partial x_i} \right) + \frac{2}{3}\delta_{ij} \left(\rho v_t \frac{\partial u_k}{\partial x_k} + \rho K_A \right) \tag{3}$$

where $v_t = s_A K_A^{1/2} 0.09$ with s_A representing the size scale of the A turbulence structures and K_A being the turbulent kinetic energy of the A scale. R_{ij_B} is calculated using (3) except K_A and s_A are replaced by K_B and s_B. Currently R_{ij_C} is set equal to $0.2R_{ij_B}$. In (2d) $\sigma_c = s_C 0.2 R_{ij_B} (0.2K_B)^{1/2}$ with s_C representing the size scale of the smallest fuel elements.

The turbulence kinetic energy of the A scale is expressed by the following relationship

$$\begin{aligned} \frac{\partial \rho G K_A}{\partial t} + \nabla \cdot (\mathbf{v} G \rho K_A) =& G - R_{il}\frac{\partial u_i}{\partial x_l} + G\frac{2}{3}C_{DR}\frac{\partial}{\partial x_l}\left[s_A \frac{R_{lk}}{K^{1/2}} \frac{\partial K_A}{\partial x_k} \right] - \\ & G\frac{K^{1/2}}{s_A} K_A - G\frac{3}{8} C_D \frac{\rho K_A K^{1/2} \alpha_s}{s_B} \end{aligned} \tag{4}$$

The first term on the left hand side represents shear generated turbulence. The second term on the left hand side represents self diffusion. The third term on the left hand side represents an energy cascade term and the last term represents the removal of turbulent energy from the A scales due to the drag in the forest. For the transport of K_B there are two additional drivers that describe the creation of turbulence at the B scale, due to the break up of turbulence at the A scale and to the mean flow in the vegetation. These source terms are

$$\frac{\partial \rho G K_B}{\partial t} = \ldots + G\frac{3}{8} C_D \frac{\rho K^{1/2} K_A \alpha_s}{s_b} + G\frac{3}{8} C_D \frac{\rho |\, u \,|^3 \alpha_s}{s_B} \tag{5}$$

Excluding parameterized forcing terms the basic algorithm for integrating (1) on a discrete mesh is second-order-accurate in space and time. The chosen mesh is one in which all variables are defined at the same grid position, A-grid. The model uses the method of averaging technique (Reisner and Kao 1997, Nadiga et al. 1996, Madala 1981)

to efficiently filter out sound waves from the compressible equation set. Employing this technique the discretized equation set can be expressed as follows:

$$u_i^{n+1} = MPDATA(u_i^n, \bar{\alpha}_{i\pm 1/2e_I}^{n+1/2}, G_i) + DONOR(\bar{R}_x^{n+1/2}, 0.5\bar{\alpha}_{i\pm 1/2e_I}^{n+1/2}, G_i) + f_x \tag{6a}$$

$$v_i^{n+1} = MPDATA(v_i^n, \bar{\alpha}_{i\pm 1/2e_I}^{n+1/2}, G_i) + DONOR(\bar{R}_y^{n+1/2}, 0.5\bar{\alpha}_{i\pm 1/2e_I}^{n+1/2}, G_i) + f_y \tag{6b}$$

$$w_i^{n+1} = MPDATA(w_i^n, \bar{\alpha}_{i\pm 1/2e_I}^{n+1/2}, G_i) + DONOR(\bar{R}_z^{n+1/2}, 0.5\bar{\alpha}_{i\pm 1/2e_I}^{n+1/2}, G_i) + f_z \tag{6c}$$

$$\theta_i^{n+1} = MPDATA(\theta_i^n, \bar{\alpha}_{i\pm 1/2e_I}^{n+1/2}, G_i) + f_\theta \tag{6d}$$

$$\rho_i^{n+1} = MPDATA(\rho_i^n, \bar{\alpha}_{i\pm 1/2e_I}^{n+1/2}, G_i) + f_\rho \tag{6e}$$

$$\rho K_{A_i}^{n+1} = MPDATA(\rho K_{A_i}^n, \bar{\alpha}_{i\pm 1/2e_I}^{n+1/2}, G_i) + f_{K_A} \tag{6f}$$

$$\rho K_{B_i}^{n+1} = MPDATA(\rho K_{B_i}^n, \bar{\alpha}_{i\pm 1/2e_I}^{n+1/2}, G_i) + f_{K_B} \tag{6g}$$

where the bar quantities are calculated by the following

$$\bar{\psi} = \frac{1}{\Delta t}\int_t^{t+\Delta t} w^i \psi^i dt \tag{7}$$

with ψ representing either the advective velocities, α, or the forcing terms, R_i, calculated in a series of first-order predictor steps (Reisner and Kao 1997). Only pressure gradient, Coriolis, and bouyancy forces are included in R_i. The integral weighting factors are not constant during the predictor steps with the weighting factors typically being biased to give a ψ which is closer to $n+1$ than n. The temporal averaging technique enables a time-step to be used in the second-order advection scheme $MPDATA$ that is usually an order magnitude larger than what is used in a compressible code without temporal averaging. The nonoscillatory forward-in-time algorithm, $MPDATA$, (Smolarkiewicz and Grabowski 1990) is used to advect all variables. Note, the monotonicity constraints in $MPDATA$ have been modified (Schar and Smolarkiewicz 1996) to ensure that scalar variables in the compressible system remain monotone. The $DONOR$ cell step in (5) is required to ensure second-order accuracy of the forcing terms (Smolarkiewicz and Margolin 1993). The turbulence terms and the heating term are not averaged in time with these terms being approximated to the first-order. Because a first-order explicit diffusion routine is used for some of the

forcing terms in FIRETEC, several of the turbulence terms within FIRETEC require subcycling for numerical stability.

The BEHAVE MODEL

The BEHAVE-like model uses the volume-of-fluid or VOF method (Margolin et al. 1997) to track the movement of a fireline across a computational cell. In principle, VOF is an Eulerian approach, as it does not track explicitly material interfaces. Instead, it reconstructs such interfaces using auxiliary dependent variables—the partial volume fractions of immiscible materials within computational cells. For example, a partial volume fraction of 0.5 would indicate that one half of the cell is burning with the fireline's orientation being determined by taking local gradients of the partial volume fractions (eq. 12 in Margolin et al. 1997). The fireline's location within a cell can be determined analytically given the orientation and the value of the partial volume fraction. Unlike in Margolin et al., the current application of the VOF technique does directly influence the advection of scalar quantities; does not use advective velocities to advect the interface; and does not conserve total volume. The conservation of total volume would not be expected in a fire which is growing in time. The current implementation of the VOF method uses spread rate information obtained from BEHAVE to move the interface. The empirical formulae (Rothermel 1972, 1991) use information such as wind speed, terrain slope, fuel moisture content, and fuel type to determine spread rate and intensity of the fire.

Instead of directly coding the formulae into our code, we have chosen to use lookup tables to determine spread rate information. The steps involved in moving the interface are as follows:

1) Flag grids cell which contain an interface or are in the vicinity of an interface.
2) Within flagged cells compute quantities needed for the lookup table: Wind speed, spread direction or the normal direction to the interface with respect to the terrain direction (e.g., interface moving up a slope), and the angle of the wind with respect to the terrain direction. Quantities needed for the lookup table such as terrain slope, fuel type, and fuel moisture content need not be calculated every time step.
3) Call the look up table and determine the individual components of spread by multiplying the spread rate by the angle associated with the direction of spread.
4) Use the individual spread rate components in a donor-cell advection scheme to move the fireline. In the above approach a split form is used to advect the interface. To minimize splitting errors the starting directions for the 1-D sweeps are alternated. Also, the code contains logic to allow for the interface to not move into grid cells which have been previously burned.

The time rate of change of the partial volume fraction multiplied by the fire intensity is used to estimate the burn rate. For each grid cell there usually is more than

one burn rate with the summation of the burn rates being equal to the total heat, H, released in the grid cell. Each burn rate is assigned a start time, t_o, and relative to that start time a particular burn rate is damped by $\exp(t - t_o)\alpha_t$. As will be shown later the comparison of HIGRAD/BEHAVE with HIGRAD/FIRETEC will provide guidance as to the value of α_t. Vertical distribution of H is accomplished by dividing H by the number of cells in the canopy.

THE FIRETEC MODEL

As stated in Linn (1997) FIRETEC takes the extremely complicated combustion physics which occur during a wildfire and simplifies these complex processes into a "universal reaction rate"

$$F = c_F \frac{\rho_f \rho_o \sigma_{cm} \Psi}{\rho_r e f s^2} \lambda \tag{8}$$

where c_f is a combustion parameter, ρ_f is the density of the fuel, ρ_o is the density of oxygen, σ_{cm} is a measure of the turbulent intensity, Ψ is the volume fraction of the region that is above critical ignition temperature as described by the temperature probability density function, and s is the scale of the smallest fuel elements. The form of λ is

$$\lambda = \frac{\rho_f \rho_o}{\left(\frac{\rho_f}{N_f} + \frac{\rho_o}{N_o}\right)^2} \tag{9}$$

The universal reaction rate appears in the H term in (1f) with the reaction rate as well appearing in the density equation, f_ρ, in an additional continuity equation for oxygen, and in a equation which predicts the temperature of the fuel.

DESIGN OF THE NUMERICAL SIMULATIONS

The simulations have been designed to demonstrate both the second-order numerics of HIGRAD and how FIRETEC can be used to possibly develop better point functionals for fire spread and/or intensity. For the HIGRAD/FIRETEC simulations the domain size was 400 m in horizontal and 120 m in the vertical. 201 $\times$ 61 grid points were used in the simulations. Environmental temperature and density profiles were chosen to be constant in space with values of $300K$ and 1.11 kg m^{-3} being used in the simulations. Four simulations were conducted with HIGRAD/FIRETEC. Three of the simulations differed only in the strength of the upstream wind velocity, with EXPF1, EXPF2, and EXPF3 using upstream wind speeds of 2,4, and 6 m s^{-1} respectively. EXPF4 used an upstream wind speed of 4 m s^{-1}, but only a first-order version of MPDATA was used in the simulation. Simulations used a time step of 0.05 s with the simulations being run for a time period of 600 s. The fire was initialized by placing a temperature perturbation of 100 K over the ambient 20-24 m from the left boundary and 2-10 m from the surface. Constants, such as s_A, and initial conditions, such as the profile of the fuel bed, are the

same as specified in chapter 5 of Linn (1997) and in a companion paper by Linn and Harlow in the proceedings for this conference.

For the HIGRAD/BEHAVE simulations the setup was almost identical to the HIGRAD/FIRETEC simulations; except, unlike the HIGRAD/FIRETEC simulations, 41×31 grid points were used in the simulations. A constant grid increment of 10 m was specified in the horizontal, but a variable grid was used in the vertical. The lower resolution of the HIGRAD/BEHAVE simulations was by design—the HIGRAD/BEHAVE model was intended to provide quick estimates of quantities such as fire spread and intensity. Though several HIGRAD/BEHAVE simulations were conducted, only two will be shown. The two simulations, EXPB1 and EXPB2, are identical expect for the values of α_t used during the runs. For EXPB1/EXPB2 α_t was set to 0.1/0.01 s^{-1} respectively. An upstream windspeed of 4 m s^{-1} was used during the simulations. For the BEHAVE-like simulations, the fire was initialized by placing a temperature perturbation of 100 K over the ambient 40 m from the left boundary and 2-10 m from the surface. For these two simulations both spread rate information and H were estimated from comparable HIGRAD/FIRETEC simulations. Hence, we will attempt to illustrate how HIGRAD/FIRETEC can be used to finetune α_t.

RESULTS

Fig. 1 illustrates the importance of second-order numerics with respect to the structure of a fire, the intensity of a fire, and the spread of a fire. The firefront progressed approximately 100 m farther downstream in EXPF4 than EXPF2. As evident in Fig. 1b the second-order numerics found in EXPF2 allow for the more frequent production of small-scale eddies which tend to disrupt the downwind transport of heat. At least for this particular set of simulations, the increased accuracy of the second-order numerics appears to offset the slight increase in computational cost.

The dependence of the spread of the fireline on the magnitude of the upstream flow velocity is shown in Fig. 2. To the first approximation the figure suggests that the spread rate— determined when the temperature in the canopy for a given column exceeds 400 K—is strongly dependent on the magnitude of the upstream wind speed and only weakly dependent on other factors such as the local magnitude of the wind speed. For example, Fig. 3 shows the average flow velocity immediately behind the flame front for EXPF3. The average being taken over a 10×10 m^2 area. The fluctuations in wind speed are quite large and appear not to be correlated with the spread rate. Another interesting item is the average rate of spread appears to be linearly proportional to the upstream wind speed. This finding is similar to the finding of Catchpole et al. (1998); however, their wind tunnel data was for upstream winds < 3 m s^{-1}.

Using the spread rate information found in Fig. 2, our HIGRAD/BEHAVE-like simulations with varying α_t are shown in Fig. 4. As evident in Fig. 4 the value of α_t

can have a large influence on the spatial extent and intensity of the temperature field associated with a simulated wildfire. Clearly, EXPB1 produces a temperature field which is much weaker than what is shown in Fig 1b. The value of H, about 50 K s^{-1} in EXPB1, could be raised to produce higher temperatures; however, the horizontal extent of the higher temperature perturbations will still be limited due to the small value of α_t which is used. EXPB2 produces a temperature field both in spatial extent and intensity which is closer to the results in Fig. 1, especially Fig. 1a, and is the preferred value of α_t for this particular setup. The value of α_t and H is dependent on factors such as wind speed, and this dependence will be investigated in the future.

CONCLUSIONS

The results of this study clearly suggest that like wind tunnel experiments FIRETEC can be used to develop point functional models for fire spread and intensity. Over the next several years we plan to validate HIGRAD/FIRETEC against controlled burns (see a companion paper in the conference proceedings by Bossert et al. concerning this issue). Once validated, HIGRAD/FIRETEC could be run over a range of environmental conditions, fuel types, moisture contents, ect.. , to establish look up tables for simple point functional models.

A important question which was only partially addressed in this study concerns the importance of local winds on the spread of the fire. For flat terrain and a homogeneous fuel bed, this study suggests that the spread of the fire is primarily dependent on the mean upstream wind. It is doubtful that the spread rate is independent of local wind in regions of complex terrain, but the ability to parameterize how the local-scale wind variations influence fire spread may be difficult. By comparing against HIGRAD/FIRETEC simulations, we plan to investigate the utility of using a point-functional model in regions of complex terrain.

A final remark concerns the need to further development the point-functional model approach. The HIGRAD/BEHAVE simulations were about an order of magnitude faster than the HIGRAD/FIRETEC simulations. If future research suggests that the fire spread is relatively independent of local winds even over complex terrain, then the BEHAVE model can be essentially decoupled from the dynamical model. The decoupling will allow the BEHAVE-like simulations to run several orders of magnitude faster than HIGRAD/FIRETEC. Thus, providing a quick first guess of fire spread.

REFERENCES

Andrews, P.L., and C.H. Chase, 1989:BEHAVE:Fire Behavior Prediction and Fuel Modeling System–Burn Subsystem Part 2, NFES 0277, National Intergency Fire Center, 3822 S. Development Ave., Boise, Idaho 83705.

——, 1986: BEHAVE:Fire Behavior Prediction and Fuel Modeling System–Burn subsystem, Part 1. Gen. Tech. Rep. INT-194. Ogden, UT:U.S. Department of Agriculture, Forest Service, Intermountain Research Station. 130 p.

Catchpole, W.R., E.A. Catchpole, B.W. Butler, R.C. Rothermel, G.A. Morris, and D.J. Latham, 1998: Rates of spread of free-burning fires in woody fuels in a wind tunnel. *Combust. Sci. and Tech.*, **131**, 1-37.

Davies, H.C., 1983: Limitations of some common lateral boundary schemes in regional NWP models. *Mon. Wea. Rev.*, **111**, 1002-1012.

Linn, R.R., 1997: A transport model for prediction of wildfire behavior. Ph.D. Dissertation, New Mexico State University; also published as Los Alamos National Laboratory Report LA-13334-T.

Linn, R., and F.H. Harlow, 1998:FIRETEC: A transport model for investigating self-determining wildfire. Second Symposium on Fire and Forest Meteorology. 11-16 January 1998, Phoenix Convention Center, Phoenix Arizona.

Madala, R. V., 1981: Efficient time integration schemes for atmosphere and ocean models. *Finite-difference Techniques for Vectorized Fluid Calculations*, D. Book, Ed., Springer-Verlag, 56-74.

Margolin, L., J. Reisner, and P.K. Smolarkiewicz, 1997: Application of the volume-of-fluid method to the advection-condensation problem. *Mon. Wea. Rev.*, **125**, 2265-2273.

Nadiga B.T., Hecht M.W., Margolin L.G., and P.K. Smolarkiewicz, 1996: 'Preliminary aspects of the method of averaging for the numerical treatment of multiple time sca systems', LA-UR-96-2409.

Reisner, J., and C.-Y.J. Kao, 1997: Application of simple numerical techniques for increasing the efficiency of a forward-in-time shallow water code on a sphere. *Parallel Computational Fluid Dynamics Algorithms and Results Using Advanced Computers*, Elsevier, New York.

Rosenkrance et al., 1994:Interagency report on the South Canyon fire–accident investigation team. Bureau of Land Management and USDA Forest Service.

Rothermel, R.C., 1991:Predicting the behavior and size of crown fires in the Northern Forests. USDA Forest Service Research Paper INT-438, Intermountain Forest and Range Experiment Station, Ogden, UT.

Rothermel, R.C., 1972:A mathematical model for predicting fire spread in wildfire fuels. USDA Forest Service Research Paper INT-115, Intermountain Forest and Range Experiment Station, Ogden, UT.

Schär, C., and P.K. Smolarkiewicz, 1996:A synchronous and iterative flux-correction formalism for coupled transport equations. *J. Comput. Phys.*, **128**, 101-120.

Smagorinsky, J. 1963:General circulation experiments with the primitive equations. I. The basic experiment. *Mon. Wea. Rev.*, **91**, 99-164.

Smolarkiewicz, P.K., and L.G. Margolin, 1997: On forward-in-time differencing fo r fluids: An Eulerian/semi-Lagrangian nonhydrostatic model for strati fied flows. *Atmos.-Ocean*, in press.

____, and ____, 1994: Variational solver for elliptic problems in atmospheric flows. *Appl. Math. and Comp. Sci.*, **4**, 527-551.

____, and ____, 1993: On forward-in-time differencing for fluids: extension to a curvilinear framework. *Mon. Wea. Rev.*, **121**, 1847-1859.

____, and W.W. Grabowski, 1990: The multidimensional positive definite advective transport algorithm: Nonoscillatory option. *J. Comput. Phys.*, **86**, 355-375.

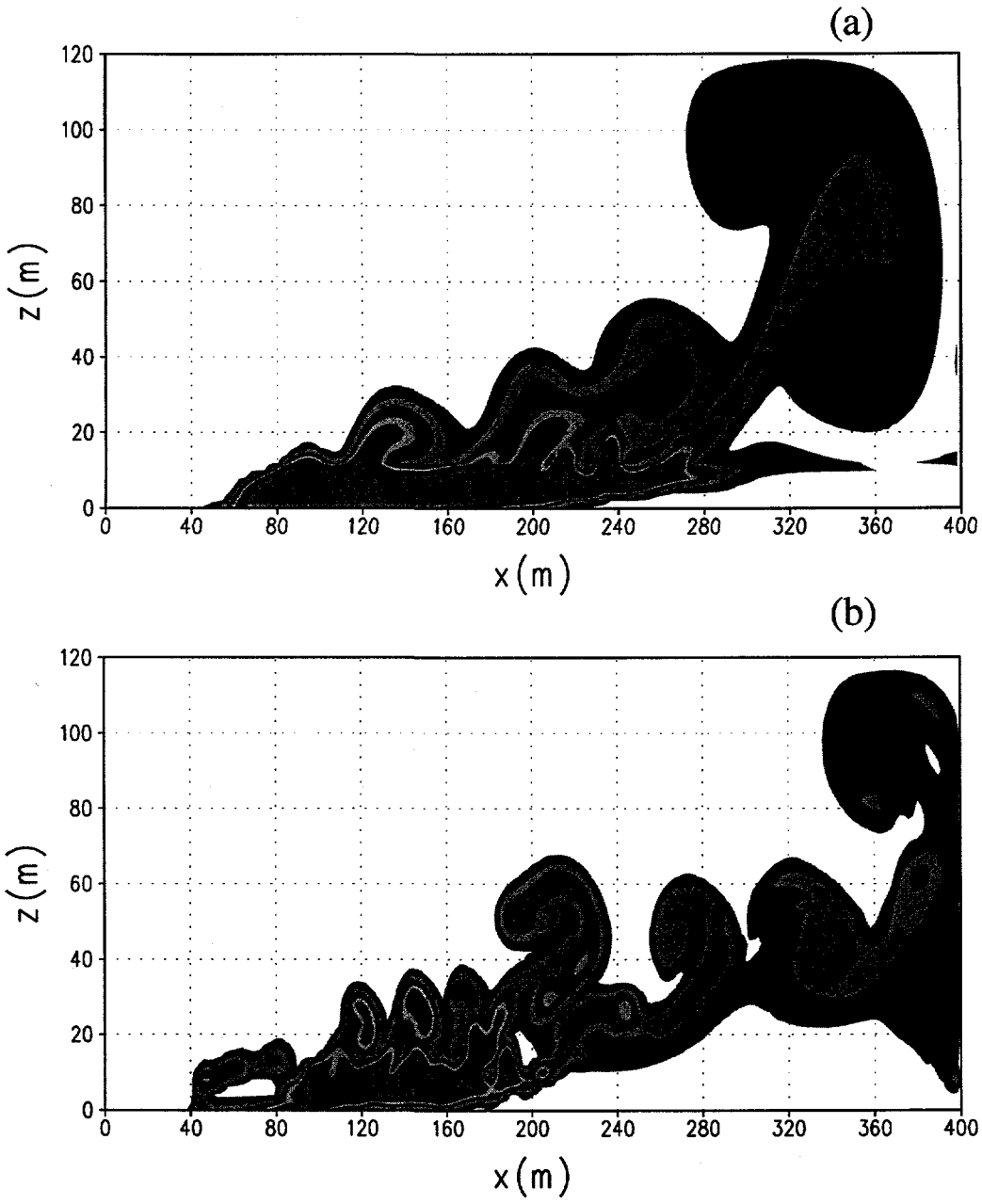

Fig. 1 Potential temperature field at 6 min. from (a) EXPF4 and (b) EXPF2.

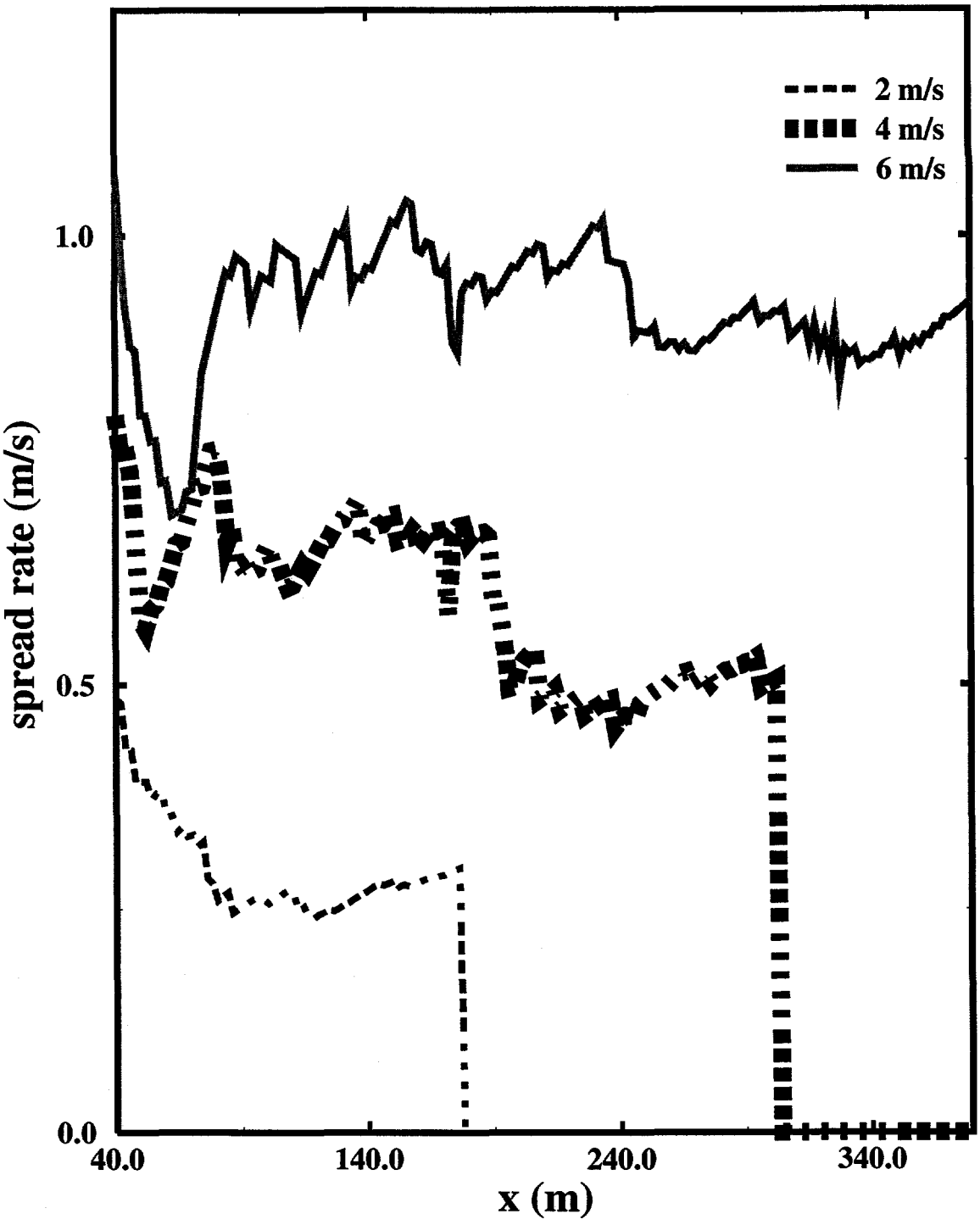

Fig. 2 Spread rate at different locations in the horizontal for EXPF1 (light dashed line), EXPF2 (heavy dashed line), and EXPF3(solid line).

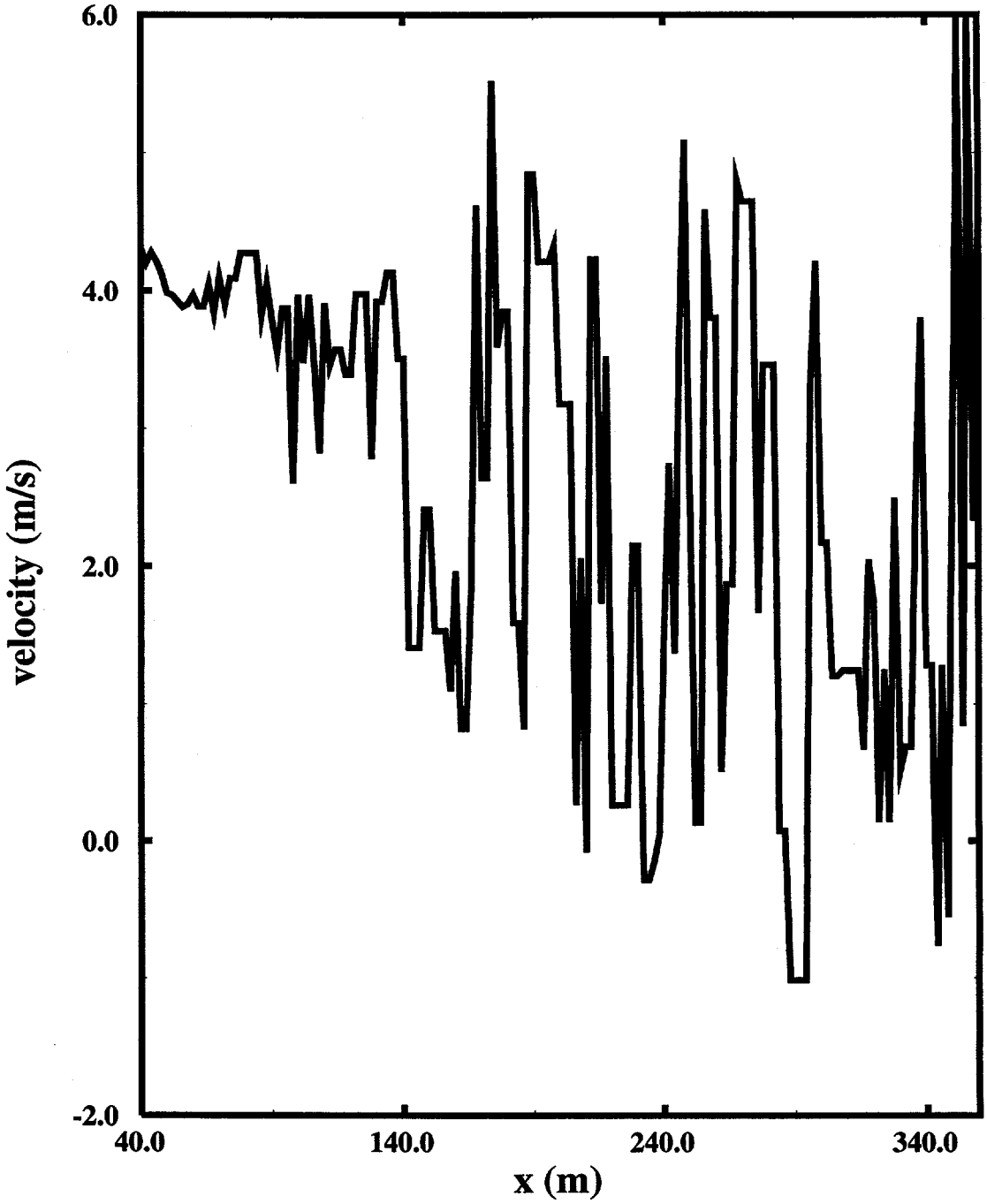

Fig. 3 Average wind velocity from EXPF3 over a 10 m by 10 m area as a function of horizonal position. Wind velocity was obtained immediately downstream of the firefront.

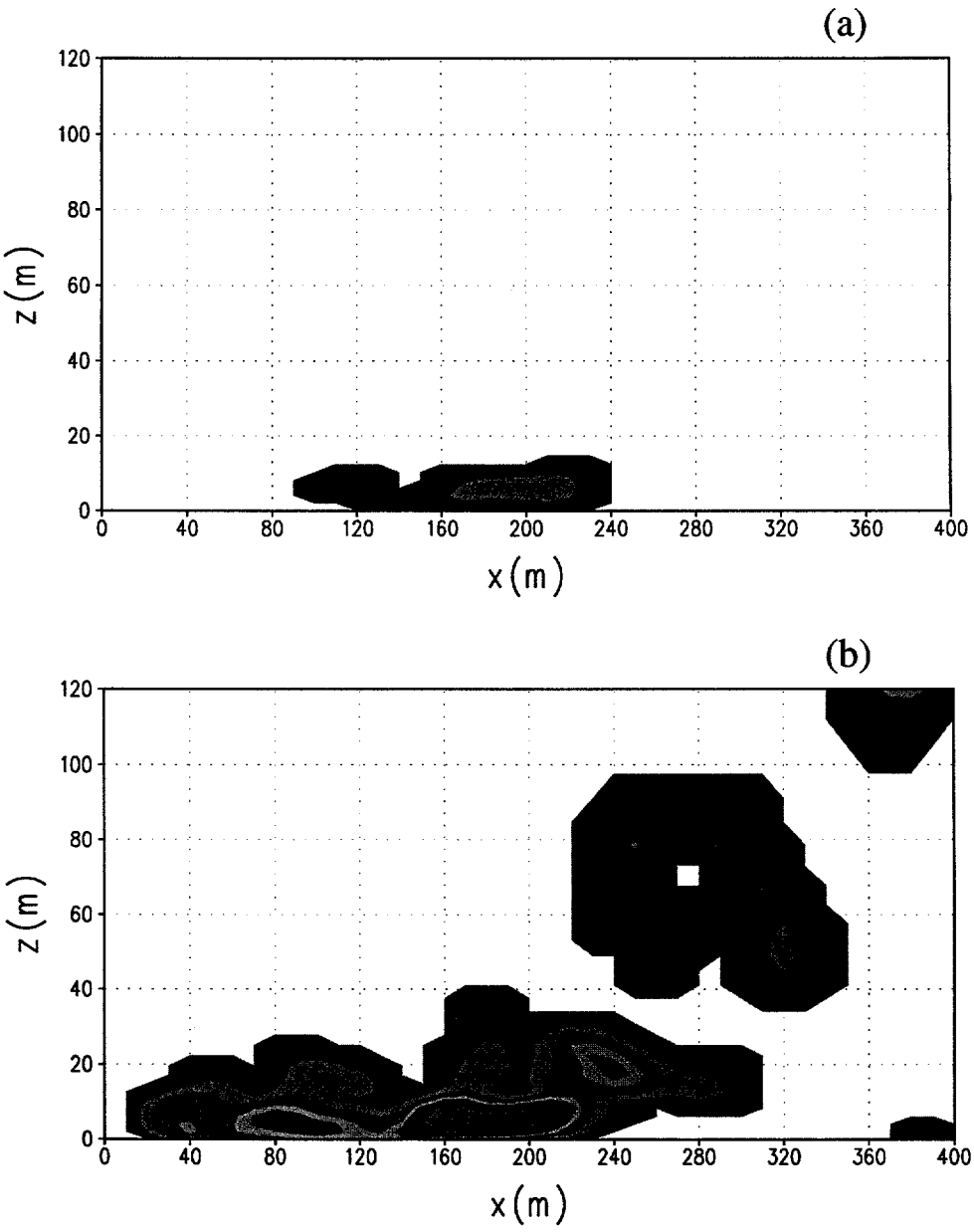

Fig. 4. Potential temperature field at 6 min from (a) EXPB1 and (b) EXPB2.